

Optimization of Fast Acquisition Methods for Whole-Brain Relative Cerebral Blood Volume (rCBV) Mapping With Susceptibility Contrast Agents

Lei Hou, PhD, Yihong Yang, PhD, Venkata S. Mattay, MD, Joseph A. Frank, MD, and Jeff H. Duyn, PhD

Fast gradient-echo magnetic resonance scan techniques with spiral and rectilinear (echoplanar) k-space trajectories were optimized to perform bolus-tracking studies of human brain. Cerebral hemodynamics were studied with full brain coverage, a spatial resolution of 4 mm, and a temporal resolution of 2 seconds. The sensitivity of the techniques to detect image signal-intensity changes during the first pass of the contrast agent was studied at a range of TEs using dedicated experiments. For single-shot versions of spiral scanning and echoplanar imaging techniques with a 0.1-mmol/kg injection of gadolinium diethylenetriamine pentaacetic acid using a mechanical injector at 10 mL/sec under 1.5 T, the maximum sensitivity was obtained at TEs between 35 and 45 msec. At TEs less than 35 msec, signal-intensity artifacts were observed in the images. Analysis of the point-spread function revealed that susceptibility changes induced by the contrast agent can result in signal shifts to neighboring voxels. These artifacts are attributed to susceptibility-related signal changes during the acquisition window. J. Magn. Reson. Imaging 1999;9:233-239. © 1999 Wiley-Liss, Inc.

Index terms: CBV; perfusion; bolus tracking (BT); spiral imaging; EPI

Abbreviations: rCBV = relative cerebral blood volume, rCBF = regional cerebral blood flow, MTT = mean transit time, BT = bolus-tracking, SPI = spiral imaging, EPI = echoplanar imaging, TACQ = duration of the data-acquisition window, PSF = point-spread function, RF = radiofrequency, MV = multi-vessel, SV = single-vessel, Gd-DTPA = gadolinium diethylenetriamine pentaacetic acid, FOV = field of view, FA = flip angle, TIP = time to peak, TOF = time-of-flight.

MAPPING OF RELATIVE CEREBRAL BLOOD VOLUME (rCBV) in human brain allows the assessment of abnormalities in cerebral hemodynamics under pathologic conditions (1,2) as well as the indirect detection of local changes in neuronal activity (3,4). One way to obtain an rCBV map with magnetic resonance imaging (MRI) is by injecting a susceptibility contrast agent such as a gadolinium chelate intravenously while monitoring image-intensity time course with a sequential imaging experiment (5). The intensity time course can be used to

estimate rCBV(5) and possibly regional cerebral blood flow (rCBF) (6) and mean transit time (MTT) (6).

Tracking of the contrast agent bolus during its first passage through the cerebral vasculature requires image acquisition with a high temporal resolution. This poses great challenges for the image-acquisition technique as well as the scanner hardware, in particular in studies requiring large volume coverage. Recent developments in fast MRI sequences and improvements in scanner hardware have allowed bolus-tracking (BT) studies with large brain coverage (7). Emerging candidates for BT studies are spiral imaging (SPI) (8) and echoplanar imaging (EPI) (9) because of their high temporal resolution and sensitivity. The latter can be optimized by adjusting TE, which affects both the size of the observed signal change (10) and the temporal stability of the image intensity (11).

Despite these attractive features of EPI and SPI, a potential problem with these techniques is the increased contribution of artifacts resulting from the susceptibility changes induced by the contrast agent. Susceptibility-related signal changes during data acquisition can result in shifting of signal intensity across the image, which can lead to errors in the calculated hemodynamic parameters. The contribution of these artifacts, together with the sensitivity, is dependent on acquisition parameters, particularly the TE and the duration of the data-acquisition window (TACQ). The purpose of the current study is to determine this dependency systematically by both dedicated gradient-echo MR experiments and theoretical analysis of the point-spread function (PSF).

MATERIALS AND METHODS

Simulations

To investigate the effects of susceptibility changes on gradient-echo SPI and EPI, a series of computer simulations was performed. The TE was counted from the center of the radiofrequency (RF) excitation to the center of the SPI/EPI readout (equivalent to the position of the data-acquisition window). The simulations were based on theoretical analysis of the PSF, starting from a magnetically uniform object (see Appendix). Two dis-

Laboratory of Diagnostic Radiology Research, National Institutes of Health, Bethesda, Maryland 20892.

Address reprint requests to: J.H.D., Laboratory of Diagnostic Radiology Research, National Institutes of Health, Building 10, Room B1N-256, Bethesda, MD 20892.

Received June 9, 1997; Accepted April 2, 1998.

© 1999 Wiley-Liss, Inc.

tinct cases of susceptibility changes were considered: a) a multi-vessel (MV) model, assuming a voxel with a random distribution of vessels much smaller than the voxel size; and b) a single-vessel (SV) model, with one vessel running through the center of a voxel.

For the purposes of this study, the susceptibility changes were assumed to occur within a single voxel, centrally located within the object. For ease of interpretation, the susceptibility effect on the image was divided into two components: one that results purely from the delay between RF excitation and data acquisition (TE effect), and another that results from non-zero TACQ (TACQ effect). To separate TE and TACQ effects, a "reference" simulation was performed with TACQ = 0.

For the MV model, an exponential signal decay was assumed with the time constant ($T2^*$) changing from 70 msec before bolus passage to 15–25 msec (see Results and Discussion: MR Experiments) during bolus passage. The maximum intravascular frequency shift considered in the SV model was around 100 Hz. This shift size was calculated from an expected maximum gadolinium chelate concentration of 18 mM (12), using an empirically determined susceptibility of 2.5 Hz/mM (13), and corrected for the orientation of the compartment. Simulations were performed on Sun-SPARC10 (Sun Microsystems, Mountain View, CA) workstations using IDL processing software (Research Systems, Boulder, CO). The calculations used a resolution of 16 points per voxel dimension and assumed cosine bell k-space apodization.

MR Experiments

The TE dependence of sensitivity and the contribution of intensity artifacts were studied within a single BT experiment to avoid variability in the injected contrast bolus characteristics. This was done, during the acquisition of a volume, by sequentially increasing TE across the individual slices in time steps of 3.5 msec, starting at the minimum achievable TE of 15.5 msec for SPI and 25 msec for EPI (TE counted to the center of data acquisition). To minimize confounding effects caused by changes in T1-weighting, the time resolution (acquisition time for each volume) was kept constant at 2 seconds in both SPI and EPI. This resulted in TR per slice of 100 msec for the 20-slice SPI volume and 112 msec for the 18-slice EPI volume.

The MRI studies were performed on normal subjects ($n = 6$ for SPI and $n = 4$ for EPI) on a 1.5-T MR unit (General Electric, Milwaukee, WI) equipped with a combined RF and gradient insert coil (Medical Advances, Milwaukee, WI). The maximum available gradient strength was 22 mT/m. A dose of 0.1 mmol/kg of gadolinium diethylenetriamine pentaacetic acid (Gd-DTPA) solution was injected into the antecubital vein at a rate of 10 mL/sec using a mechanical injector (Spectris, Medrad, Pittsburgh, PA). The human subject protocol was approved by the intramural review board of the National Institutes of Health.

Multi-slice, single-shot, gradient-echo SPI and EPI were used to acquire axial images with a strong susceptibility ($T2^*$) contrast. The multi-slice approach was preferred to an interleaved three-dimensional acquisition

for superior temporal stability (8), reduced sensitivity to T1 effects, and reduced blurring related to signal changes during data collection. The SPI and EPI gradient waveforms were designed to have minimum duration; for the SPI waveforms, this was achieved with a slew-rate limited design. Using a maximum slew rate of $120 \text{ T}\cdot\text{m}^{-1}\cdot\text{sec}^{-1}$, this led to a duration of 22 msec for SPI and 41 msec for EPI (equivalent to TACQ). Other acquisition parameters were: field of view (FOV) 24 mm, slice thickness 4 mm, matrix size 64×64 , 240 mm FOV, flip angle (FA) 82° (Ernst angle for gray matter). Total measurement time for each BT experiment, consisting of 40 sequential scans, was 80 seconds.

To assess the feasibility of obtaining whole-brain maps of hemodynamic parameters such as rCBV and time to peak (TTP), SPI BT experiments were performed with optimal parameter settings (TR 58 msec, FA 82° , TE 36 msec), as determined from the preceding experiments. The shortest possible TR was chosen to allow 34-slice whole-brain coverage with a time resolution (scan time per volume) of approximately 2 seconds. For anatomic reference, time-of-flight (TOF) images were acquired using spoiled gradient-echo technique, with TE/TR/FA of 10 msec/50 msec/ 60° .

Data Analysis

Data processing was performed using Sun-SPARC 10 workstations with IDL imaging data software. For the SPI data, a regridding algorithm with a gaussian convolution window was used to resample the data on an orthogonal equidistant grid. For both SPI and EPI experiments, a circular cosine bell k-space apodization was used, starting at 50% of the maximum radius. For the EPI data, ghost reduction was performed using a reference scan with the blipped gradient switched off (8).

The sensitivity of the BT experiment was calculated from the peak signal loss with bolus passage divided by the baseline signal instability. A mask based on magnitude of peak signal loss was applied to the raw data for choosing voxels in the gray matter area. The peak signal loss was determined from a three-parameter fit (7) to the signal-intensity time course. This method proved robust over the range of TEs studied and provided a good fit for the variable TE data with a relatively low signal-to-noise ratio. As an indication of signal instability, the standard deviation of the prebolus baseline signal was determined. Note that this value for the signal fluctuations (instability) includes effects such as scanner noise and tissue motion.

For the experiments performed at optimum settings of TE and TR, a four-parameter Γ -variate function (14) was used as a model for the parametric analysis. After conversion of the signal-intensity time course to a concentration time curve using the equation $S(t) = S(0) \times \exp(-k \times C(t)/TE)$, the Γ function fit followed from a least-squares difference analysis. The fit was then used to extract rCBV from the area of the peak, time to peak (arrival time), and bolus width (related to MTT) on a voxel-by-voxel basis. The bolus width was defined by the full width at half-maximum of the fitted peak.

RESULTS AND DISCUSSION

Simulations

The computer simulations using the SV and MV models showed that focal susceptibility changes affect areas in the image that extend far beyond the area of change in the object. This was the case for both TE and TACQ effects, each resulting in significant contributions to the PSF outside the central area (central voxel). The character of the image-intensity changes depended strongly on experimental parameters and was different for SPI and EPI experiments. An example of the TACQ effect is shown in Figure 1a and b for the MV model and in Fig. 1c and d for the SV model with the vessel running parallel to the static magnetic field. Note that the intensity changes affect many voxels outside the (central) voxel where the susceptibility changes occur. An

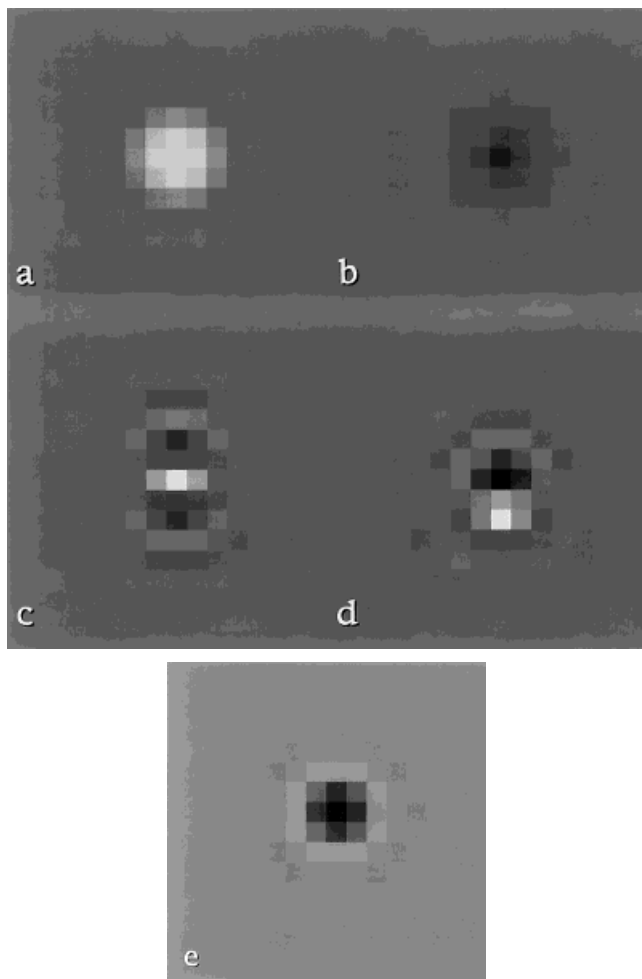


Figure 1. Image-intensity shifts caused by finite TACQ (a–d) compared with purely TE-related signal loss (TACQ = 0). The results were obtained assuming a T_2^* change from 70 to 25 msec (MV model) and a 50-Hz frequency shift (SV model) during bolus passage. The blood volume fraction was 1.6% (SV model). The intensity scales are [-0.5%, +0.5%] for (a–d) and [-50%, +50%] for (e). (a) MV model, SPI experiment with TE/TACQ = 30/22 msec. (b) SV model, SPI experiment with TE/TACQ = 30/22 msec. (c) MV model, EPI experiment with TE/TACQ = 30/41 msec. (d) SV model, EPI experiment with TE/TACQ = 30/41 msec. (e) MV model, pure TE effect, TE/TACQ = 30/0 msec.

example of the TE effect for the MV model is shown in Fig. 1e. The intensity shifts observed in this case are related to the “standard” imaging PSF and can be manipulated by the apodization function (W in Appendix) applied during image reconstruction. With the SV model, the TE effects, together with the final image intensity, strongly depend on the size of the frequency shift associated with the passage of the bolus as well as on vessel orientation and position within the voxel. This can be explained by the highly variable phase differences generated by the susceptibility changes within a voxel and is analogous to the effects discussed by Haacke et al (15) for the situation TACQ = 0.

An example of the magnitude of calculated signal shifts with EPI and SPI experiments is given in Table 1. Note that the intensity artifact in the central voxel is quite small (less than 1%, compared with a relative signal change of 46% for the pure TE effect; T_2^* 25 msec, TE 30 msec). Larger TACQ effects can be expected with larger blood-volume fractions or a higher injection dose.

The results discussed above pertain to susceptibility changes in single voxels. To estimate the effects of susceptibility changes in larger areas, PSFs of all contributing voxels need to be combined, generally leading to complex patterns of signal changes. In cases of pure exponential (T_2^*) signal decay, the size of the area (cluster) determines the actual observed signal loss with bolus passage in the central area. For SPI, this loss decreases with cluster size, corresponding to a shift of the effective T_2^* -weighting to a lower value of TE (11). An opposite and much smaller effect is observed with EPI (11).

MR Experiments

The results of varying the TE in BT experiments are displayed in Figs. 2–4. Figure 2a (SPI) and b (EPI) shows the maximum signal drop with the first passage of the contrast agent bolus, normalized to the baseline (prebolus) signal. The data for the different subjects were also normalized to the amount of contrast agent injected, which proved to give more comparable maximum signal changes. The maximum effect is reached at around TE 50–55 msec for SPI and at around TE 45 msec for EPI. The solid lines in the figures represent a two-parameter fit (difference of two exponential decays). The fits show a similar TE dependency of the signal drop for SPI and EPI data, with T_2^* values of 80 ± 20 msec for baseline and

Table 1
Calculated Signal Intensity Shifts ΔS , Generated by the Finite Duration of the Data Acquisition Window (TACQ)

	ΔS – SPI TACQ = 22 ms	ΔS – EPI TACQ = 41 ms
MV, $T_2^* = 15$	0.26%	0.48%
MV, $T_2^* = 25$	0.49%	0.35%
SV, $\Delta f = 50$ Hz	0.43%	0.66%
SV, $\Delta f = 100$ Hz	0.70%	0.61%

The numbers indicate the magnitude signal change in the central voxel, assuming a 1.6% blood volume fraction. The signal changes are relative to the baseline (pre-bolus) image intensity.

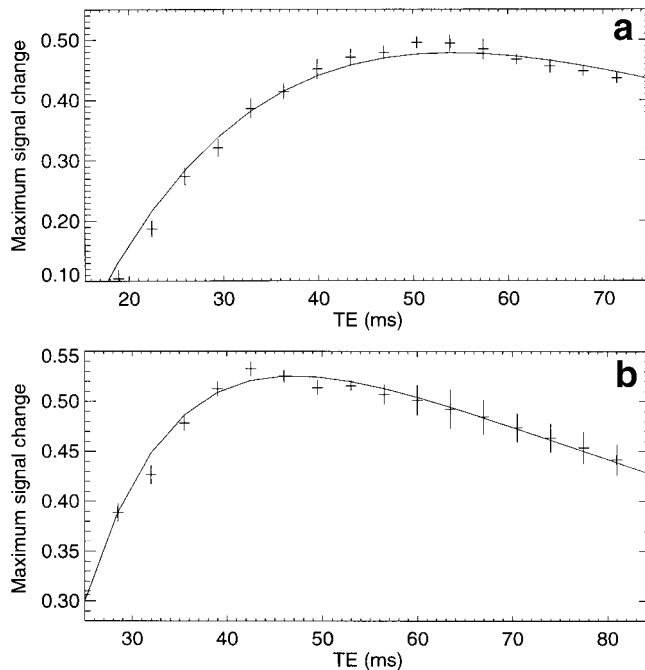


Figure 2. Maximum signal change with bolus passage in a gray matter region of interest, relative to prebolus signal. The graphs represent averages of all subjects for the SPI (a) and EPI (b) experiments, with SDs between subjects indicated with error bars. The solid line represents a fit (difference of two exponential decays) to the data.

23 ± 11 msec for the contrast bolus passage. The baseline instability increased with TE for both SPI and EPI experiments and was substantially larger for the EPI data. The increase in signal fluctuations at longer TEs is attributed to increased motion sensitivity and reduced signal-to-noise ratio. The overall sensitivity, as calculated from the maximum signal change (Fig. 2) divided by the temporal SD, is given in Fig. 3a and b for SPI and EPI, respectively. For SPI, an optimum sensitivity of 42 is found at TE 36 msec; for EPI, this value was 38 at TE 36 msec.

As predicted by the simulations (Fig. 1), some voxels showed small positive signal changes with bolus passage, and their number increased at shorter TE (Fig. 4). This resulted in a negative calculated rCBV in these voxels. The percentage of these voxels was largest for SPI (Fig. 4a). This effect is attributed to the signal shifting resulting from $T2^*$ and off-resonance effects during TACQ, as demonstrated by the simulations. At a TE of 36 msec, the optimum condition with respect to sensitivity, the effect is fairly small. On the other hand, at lower values of TE or longer TACQ, the effect can be quite large (Fig. 4b).

A potential additional source of artifacts in BT experiments is signal-intensity changes related to the shortening of the intravascular $T1$ induced by the injected contrast agent. This is an issue in experiments with significant spin saturation, eg, when $TR_{\text{effective}} < T1$ and FA is high. ($TR_{\text{effective}}$ here indicates an overall TR, ie, the number of slices times TR.) Under the current conditions with $TR_{\text{effective}} = 2$ seconds, $T1$ values of 1.2 and .8 seconds in blood and tissue (gray matter) for a 1.5-T

magnetic field (16), FA of 82° , 2% blood-volume fraction, and assuming a $T1$ of 20 msec for blood during bolus passage, by using an equation for the signal intensity in a gradient-echo pulse sequence (16), we estimated the maximum effect of the $T1$ on signal intensity to be 1.3% and therefore negligible. This was verified experimentally by reducing FA to 45° , which did not significantly change the contribution of artifacts (ie, a similar percentage of voxels showed signal increase with bolus passage).

Figure 5 shows the results of a BT experiment using a SPI pulse sequence performed with optimal parameter settings (TE = 36 msec, TR = 58 msec, single-dose injection). Displayed are rCBV (a), arrival time (time to peak) (b), bolus width (c), and TOF-weighted anatomic reference images (d). A subset of 5 slices (out of the 34) was chosen for display. As expected, a relatively high blood volume is observed (Fig. 5a) in gray matter areas and highly vascularized areas. In addition, the high contrast observed in the time-to-peak map (Fig. 5b) indicates a delayed arrival (up to 5 seconds) of the bolus in the white matter, the choroid plexus, and the larger vessels such as sinuses relative to the arrival in the arteries. The bolus width (Fig. 5c) showed no significant regional variation relative to the noise level, except for a focal increase in the choroid plexus. These results demonstrate the feasibility of performing rCBV mapping with full brain coverage and adequate signal-to-noise ratio.

In conclusion, both SPI and EPI allow for bolus-tracking experiments with full brain coverage and a

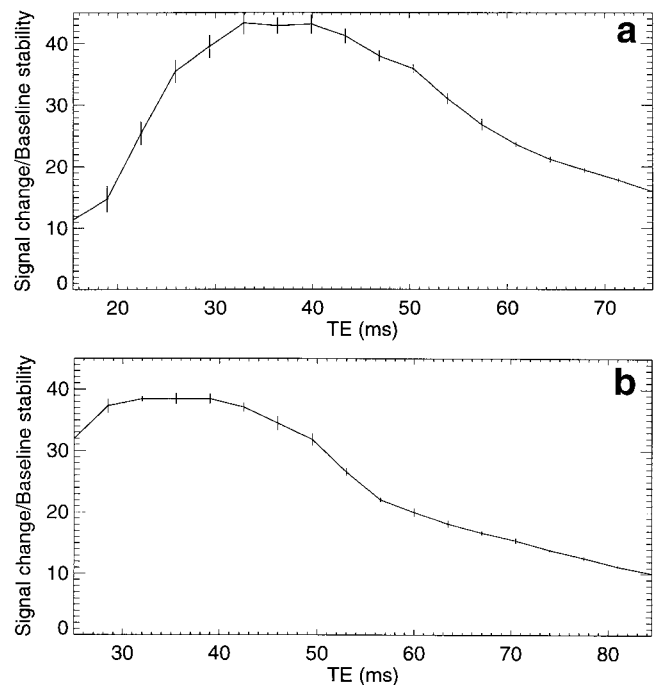


Figure 3. Sensitivity of SPI (a) and EPI (b) BT experiments as a function of TE. The sensitivity was determined from the ratio of the average signal change with bolus passage and the average scan-to-scan stability of baseline images. The error bars indicate the SDs between subjects. Both SPI and EPI experiments show a fairly flat optimum around TE = 35 msec.

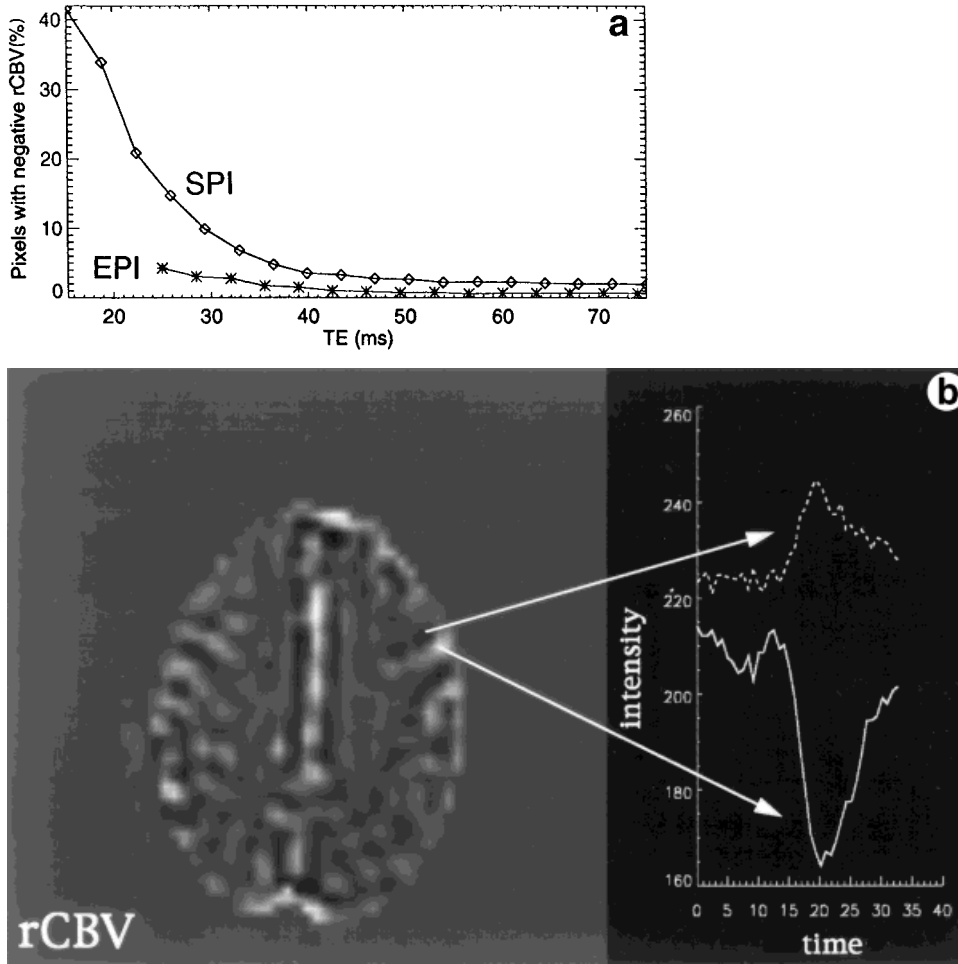


Figure 4. Image-intensity artifacts related to signal changes during TACQ. (a) Percentage of voxels with negative rCBV, as a function of TE, in SPI (diamonds) and EPI (asterisks) BT experiments. The contribution of these intensity artifacts is significantly larger with SPI than with EPI and increased dramatically at TE < 35 msec. (b) Image-intensity artifacts in an SPI BT experiment with TACQ/TE = 22/20 msec, using a 0.15-mmol/kg dose of Gd-DTPA. The conditions were chosen to amplify the effect. Specific areas in the rCBV map have neighboring voxels with opposing signal changes.

temporal resolution of less than 2 seconds. The minimum achievable temporal resolution is somewhat better with SPI. Experiments with varying TE on normal subjects for the current implementation of single-shot SPI and EPI techniques showed similar TE dependency of the sensitivity. The optimum TE value for standard dose injection was in the range of 35–45 msec for the two techniques. At shorter values of TE, image-intensity artifacts related to the non-zero duration of the data-acquisition window significantly distort the hemodynamic information, in particular with SPI.

APPENDIX

In susceptibility contrast-agent studies, the intravascular contrast agent generates a distribution of frequency shifts within the vasculature and in the surrounding tissue. This distribution is dependent on the vessel orientation and can be approximated by:

$$\Delta f_i(r, \phi, \theta) = \gamma \cdot \Delta\chi \cdot B_0 \cdot (\cos^2 \theta - 1/3), \quad (1a)$$

$$\Delta f_o(\pm r, \phi, \theta) = \gamma \cdot \Delta\chi \cdot B_0 \cdot \sin^2 \theta \cdot (\cos 2\phi) \cdot \left(\frac{R}{r}\right)^2, \quad (1b)$$

with Eqs. [1a] and [1b] for the distributions in the vasculature and the surrounding tissue, respectively.

To simulate the effects of frequency shifts on the MR image, we assume an object with an intensity distribution $S(r)$ in the absence of artifacts and without k-space signal apodization. We subdivide the image into elements (subvoxels) dr with dimensions small compared with the voxel size and compared with the spatial variation of frequency shift $\Delta f(r)$. Hence, Δf is constant over dr . For the k-space representation of $S(r)$, we find:

$$S(k) = FT^{-1}[S(r)] = \sum_{FOV} S(r') \cdot FT^{-1}[\delta(r - r')] \cdot dr', \quad (2)$$

with FT^{-1} indicating the inverse Fourier transform, and as a function that is non-zero exclusively within the subvoxel. Including the effects of apodization (W) and off-resonance and T2* effects (F), we find:

$$S'(k) = \sum_{FOV} S(r') \cdot FT^{-1}[\delta(r - r')] \cdot W(k) \cdot F(k, r') \cdot dr' \quad (3)$$

$F(k, r)$ indicates a position-dependent k-space distribution, representing effects of signal-phase dispersion during TACQ, generated by $\Delta f(r)$. Note that T2* effects can be included in $F(k, r)$ as a magnitude term, assuming that it is generated by a phase distribution that is random over dr . The resulting image intensity follows from a forward Fourier transform:

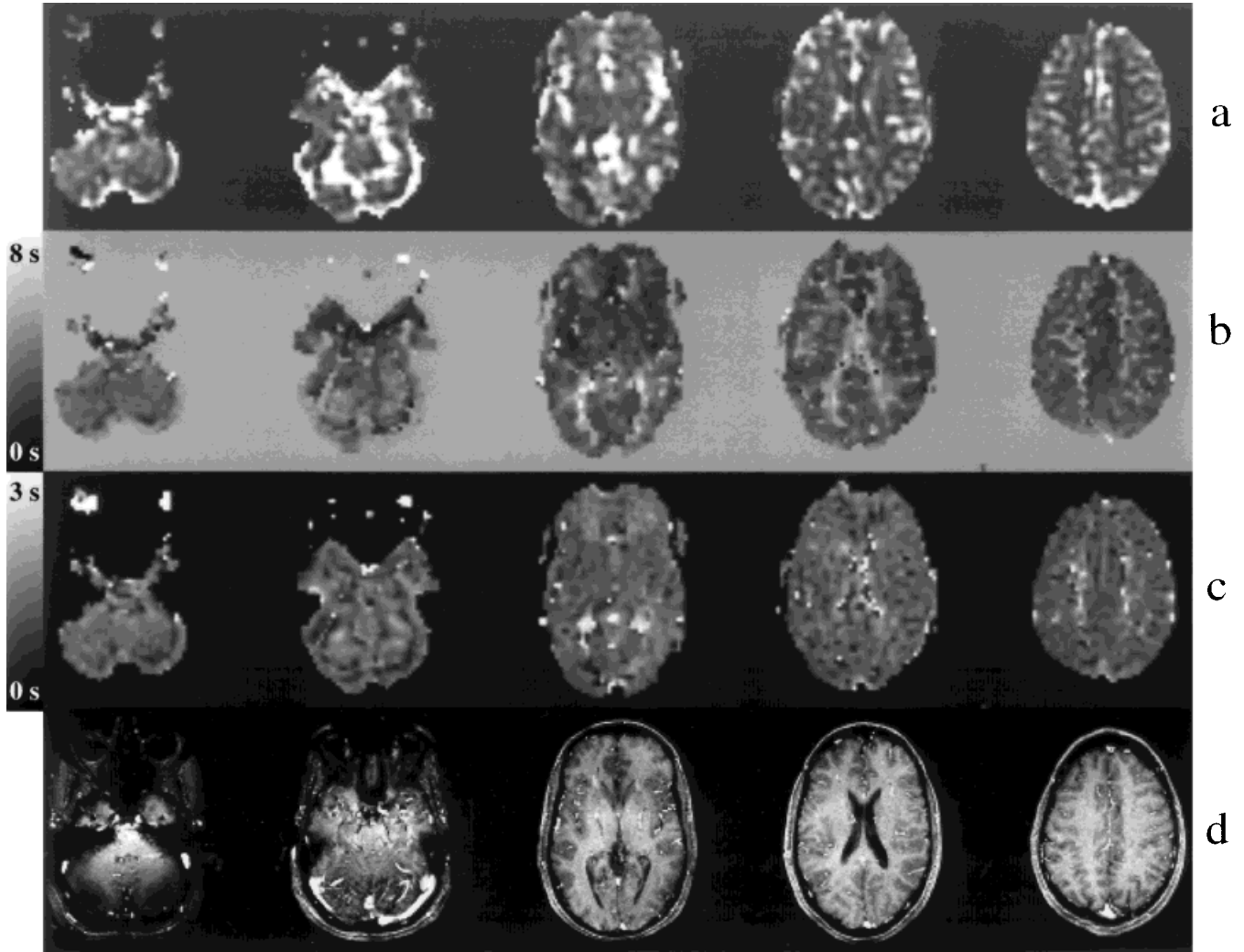


Figure 5. BT experiment on a normal subject performed under optimal parameter settings (see text). Five slices out of a 34-slice data set were selected for display, showing rCBV (a), time to peak (b), apparent mean transit time (c), and TOF reference maps (d) at an optimum TE of 36 msec. The reference images are time-of-flight maps acquired by a spoiled gradient-echo pulse sequence.

$$S'(r) = FT[S'(k)] = \sum_{FOV} FT[W(k) \cdot F(k, r')] \otimes [\delta(r - r')] \cdot S(r') \cdot dr' \quad (4)$$

The term $FT[W(k) \times F(k, r)]$ represents the PSF for the image and has a spatial dependence.

The effects of off-resonance on PSF are sequence-dependent: for EPI with the blipped gradient encoded in the y direction, we have

$$F_{EP}(k, (x, y)) = \exp(i \cdot 2 \cdot \pi \cdot (k_y + N/2) \cdot \Delta f(x, y) \cdot T/N). \quad (5a)$$

In SPI, $F(k, r)$ can be approximated by a radial distribution. For slew-rate-limited spiral trajectories (11), we have:

$$F_{SP}(k, (x, y)) = \exp(i \cdot 2 \cdot \pi \cdot (k_x^2 + k_y^2)^{0.75} \cdot \Delta f(x, y) \cdot T/N). \quad (5b)$$

ACKNOWLEDGMENTS

We thank Drs. Frank Ye and Jeff Petrella for their helpful suggestions.

REFERENCES

1. Tizzy AA, Massoth RJ, Ball WS, Majumdar S, Dunn RS, Kirks DR. Cerebral perfusion in children: detection with dynamic contrast-enhanced T2*-weighted MR images. *Radiology* 1993;187:449-458.
2. Maas LC, Harris GJ, Satlin A, English CD, Lewis RF, Renshaw PF. Regional cerebral blood volume measured by dynamic susceptibility contrast MR imaging in Alzheimer's disease: a principal components analysis. *J Magn Reson Imaging* 1997;7:215-219.
3. Belliveau JW, Rosen BR, Kantor HL. Functional cerebral imaging by susceptibility-contrast NMR. *Magn Reson Med* 1990;14:538-546.
4. Sorensen AG, Tievsky AL, Ostergaard L, Weisskoff RM, Rosen BR. Contrast agents in functional MR imaging. *J Magn Reson Imaging* 1997;7:47-55.
5. Rosen BR, Belliveau JW, Chien D. Perfusion imaging by nuclear magnetic resonance. *Magn Reson Q* 1989;5:263-281.
6. Rempp KA, Brix G, Wenz F, Becker CR, Guckel F, Lorenz WJ. Quantification of regional cerebral blood flow and volume with dynamic susceptibility contrast-enhanced MR imaging. *Radiology* 1994;193:637-641.

7. Duyn JH, Gelderen PV, Barker P, Frank JA, Mattay VS, Moonen CTW. 3D bolus tracking with frequency-shifted BURST MRI. *J Comput Assist Tomogr* 1994;18:680-687.
8. Duyn JH, Yang Y, Mattay VS, Frank JA, Hou L. Functional magnetic resonance neuroimaging data acquisition techniques. *Neuroimage* 1996;4:S76-S81.
9. Maeda M, Maley JE, Crosby DL, et al. Application of contrast agent in the evaluation of stroke: conventional MR and echo-planar MR imaging. *J Magn Reson Imaging* 1997;7:23-28.
10. Boxerman JL, Hamberg LM, Rosen BR, Weisskoff RM. MR contrast due to intravascular susceptibility perturbations. *Magn Reson Med* 1995;34:555-556.
11. Yang Y, Glover GH, Gelderen PV, et al. A comparison of fast MR scan techniques for cerebral activation studies at 1.5 Tesla. *Magn Reson Med* 1998;39:61-67.
12. Albert MS, Huang W, Lee JH, Patlak CS, Springer CS. Susceptibility changes following bolus injections. *Magn Reson Med* 1993;29:700-708.
13. Conturo T, Barker PB, Mathews VP, Monsein M, Bryan RN. MR imaging of cerebral perfusion by phase-angle reconstruction of bolus paramagnetic-induced frequency shifts. *Magn Reson Med* 1992;27:375-390.
14. Lu D, Monahan WG. Effect of sample numbers on the kinetic data analysis of MR contrast agents. *Magn Reson Med* 1993;30:131-134.
15. Haacke EM, Hopkins A, Lai S, et al. 2D and 3D high resolution gradient echo functional imaging of the brain: venous contributions to signal in motor cortex studies. *NMR Biomed* 1994;7:54-62.
16. Stark DD, Bradley WG. *Magnetic resonance imaging*. 2nd ed. Chicago: Mosby-Year Book; 1992. p 113-135.